Int J Earth Sciences (Geol Rundsch) (2002) 91 : 231–245
DOI 10.1007/s005310100208

ORIGINAL PAPER

R. Hetzel · J. Glodny

A crustal-scale, orogen-parallel strike-slip fault in the Middle Urals: age, magnitude of displacement, and geodynamic significance

Received: 20 April 2000 / Accepted: 23 February 2001 / Published online: 24 May 2001

Abstract The kinematic evolution of an orogen-parallel strike-slip fault in the Middle Urals demonstrates that orogen-parallel mass transfer was an important, previously underestimated process during the syncollisional evolution of the Middle Urals. The Kyshtym strike-slip fault extends NNE, parallel and adjacent to the Main Uralian fault, which is the main suture of the Uralide orogen. The Kyshtym fault is interpreted as one of two conjugate strike-slip fault zones that have accomodated the longitudinal transfer of material along the margins of a rigid indenter belonging to the East European craton. The dextral Kyshtym shear zone was active under retrograde lower amphibolite to middle/lower greenschist facies conditions. Four metagranitic, muscovite-bearing mylonites yielded Rb–Sr internal mineral isochron ages of 247.5±2.9, 244.5±6.5, 240.0±1.4, and 240.4±2.3 Ma, whereas a biotite-rich sample, without muscovite, gave a mineral isochron age of 229.1±3.2 Ma. The results indicate almost complete Sr-isotopic reequilibration on the hand specimen scale during mylonitization. The muscovite ages are interpreted as deformation ages and demonstrate a Late Permian/Early Triassic age for the Kyshtym shear zone. The shear zone transects a pre-orogenic syenite intrusion of Ordovician age. A maximum shear strain of γ=7±3 is estimated from the shape of the ductily deformed syenite body in map view and from the length/width ratios of deformed amphibolite bodies in the country rock. This shear strain suggests a maximum displacement of 28±12 km for the ~4-km-thick Kyshtym shear zone. A younger brittle fault, oriented subparallel to the shear zone, accomplished an additional horizontal displacement of 15±3 km; thus, the total displacement along the fault system is 43±15 km.

R. Hetzel (✉) · J. Glodny
GeoForschungsZentrum (GFZ) Potsdam, Telegrafenberg,
14473 Potsdam, Germany
E-mail: hetzel@gfz-potsdam.de

Keywords Urals · Rb–Sr · Mylonite · Ductile deformation · Tectonics

Introduction

The N/S-trending Uralide orogen (Fig. 1a) originated during the collision of the East European craton with a Siberian-Kazakhian terrane assemblage in the Late Paleozoic (e.g., Hamilton 1970; Ivanov et al. 1975; Zonenshain et al. 1984). Two major phases of orogenic shortening were separated by a period of tectonic quiescence throughout most of the Carboniferous, indicated by the deposition of shallow-water carbonates on the East European platform (Brown et al. 1997; Puchkov 1997). The first orogenic phase took place in the Late Devonian/Early Carboniferous and is characterized by the accretion of island arcs against the East European craton (Kazantseva and Kamaletdinov 1986; Echtler et al. 1997; Puchkov 1997; Brown et al. 1998). The second phase resulted in the formation of the western foreland thrust and fold belt from Early Permian until Early Triassic time (e.g., Brown et al. 1997; Giese et al. 1999).

A NW–SE shortening direction has been inferred for the first orogenic phase based on (a) NW-directed thrusting of slope-and-basin sediments and flysch deposits onto the East European craton (Giese et al. 1999), (b) NW–SE stretching lineations that formed by top-to-the-NW thrusting in the internal parts of the Middle Urals (Echtler et al. 1997), and (c) regionally developed folds with NE/SW-trending axes in high-pressure rocks of the Maksyutov complex in the Southern Urals (Echtler and Hetzel 1997; Hetzel et al. 1998). For the second, collisional phase an E–W shortening direction has been derived from the kinematic evolution of the foreland thrust-and-fold belt (Brown et al. 1997; Giese et al. 1999) and paleogeographic considerations (Puchkov 1997). Strike-slip faults that were presumably active during the upper Permian/

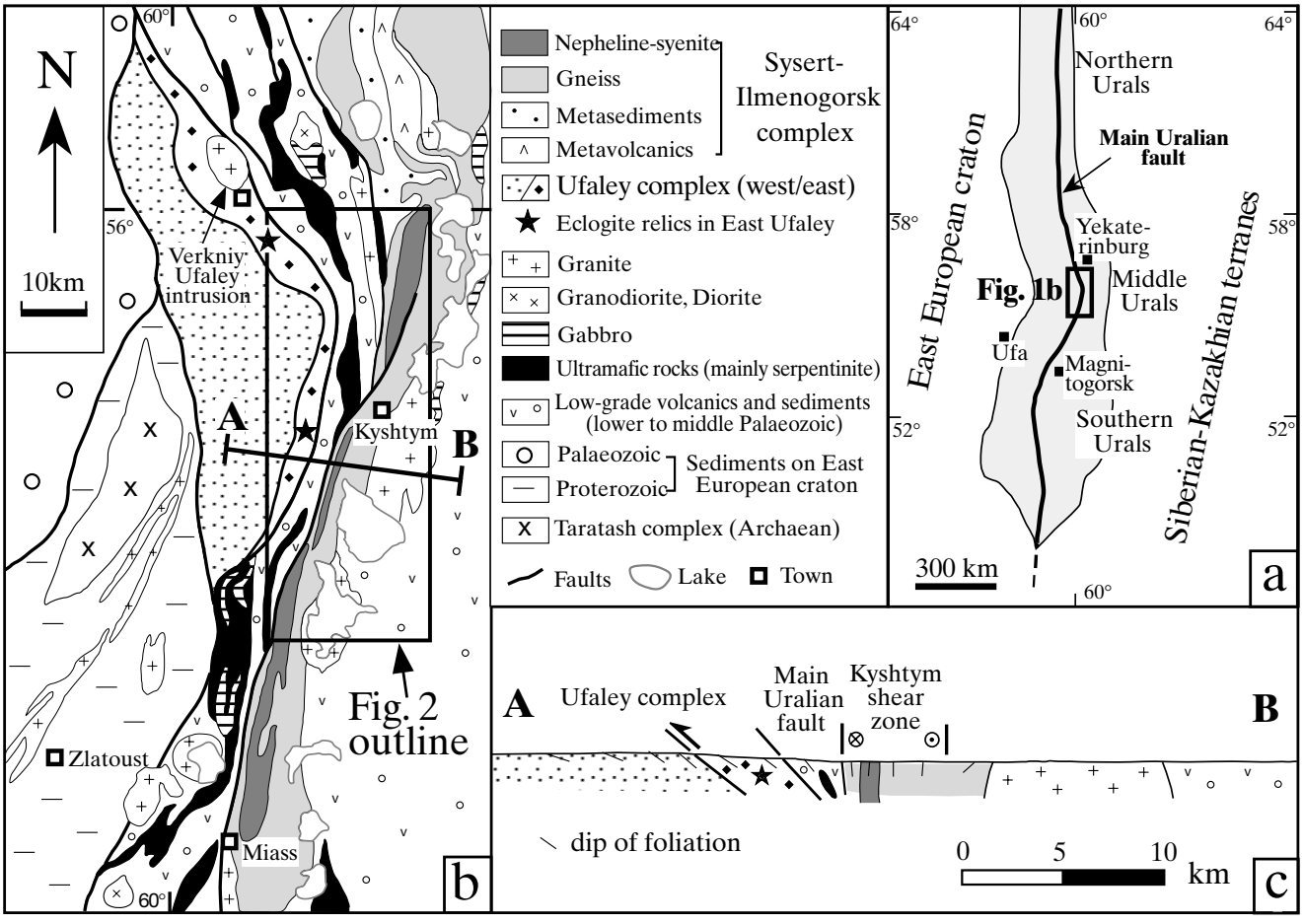

Fig. 1 **a** Map showing the N/S-trending Uralian orogen and the course of the Main Uralian fault which constitutes the boundary between the East European platform and Siberian-Kazakhian terranes. **b** Simplified geological map of the Middle Urals with the Sysert-Ilmenogorsk complex to the east, and the Ufaley complex to the west of the Main Uralian fault. The Main Uralian fault zone is characterized by abundant ultramafic rocks. Modified from Sobolev (1986). **c** Simplified cross section through the Ufaley and Sysert-Ilmenogorsk complexes. Based on Echtler et al. (1997) and own field observations

lower Triassic have only been described in the vicinity of the Main Uralian fault in the Southern Urals (Kisters et al. 1999).

This study documents the presence of a crustal-scale strike-slip fault in the Middle Urals, which reflects the transfer of material parallel to the Uralian orogen during the Permo-Triassic collisional episode. Since the metamorphic temperature during ductile deformation was below the lower temperature limit for thermally induced reopening of the Rb/Sr system in white mica, we argue that the age of the fault can be well constrained by Rb–Sr dating of muscovite-bearing mylonites. Combining a shear strain estimate for the ductile shear zone with our Rb–Sr age data offers the possibility of deriving a rough strain rate estimate for the fault. Finally, we discuss the implications of the fault for the geodynamic evolution of the Urals.

Geological setting and geodynamic evolution of the Middle Urals

The Uralian orogenic belt evolved by accretion of island arcs, microcontinents, and oceanic domains along the eastern margin of the East European craton (e.g., Hamilton 1970; Ivanov et al. 1975; Puchkov 1997; Hetzel 1999). The main suture separating the Archean/Proterozoic East European craton in the west from island arcs and microcontinents of Siberian-Kazakhian affinity in the east is known as the Main Uralian fault (Zonenshain et al. 1984; Puchkov 1997). This east-dipping fault forms a several-kilometer-wide tectonic melange including abundant ultramafic rocks (dominantly serpentinite), gabbro, and low-grade Silurian-Devonian sedimentary rock. The overall structure of the Middle Urals is characterized by a curvature of the Main Uralian fault which reflects the shape of a promontory belonging to the East European craton (Fig. 1a).

At latitude 55–57°N, the internal portion of the Middle Urals is dominated by two metamorphic complexes, the Sysert-Ilmenogorsk complex to the east

and the Ufaley complex to the west of the Main Uralian fault (Fig. 1b; Keilman 1974). The Sysert-Ilmenogorsk complex has been interpreted as a Devonian island arc that formed above an east-dipping subduction zone (Echtler et al. 1997). The arc must have been formed on older basement since igneous rocks of Early Paleozoic age are present in this zone (Ilmenogorsk-Vishnevogorsk complex; see below). The Ufaley complex is thought to represent the subducted continental margin of the East European craton (Echtler et al. 1997; Hetzel and Romer 1999). U–Pb and Sm–Nd ages from the northern part of the Sysert-Ilmenogorsk complex suggest that upper amphibolite facies peak metamorphic conditions in the Sysert-Ilmenogorsk complex were attained in Early Carboniferous time when the island arc collided with the East European craton and was internally thickened by NW-directed thrusting (Echtler et al. 1997). The subduction of the East European continental margin below the arc generated blueschists and eclogites now present at two localities in the East Ufaley complex (Fig. 1b; Belkovski 1989). The eclogites have been intensely overprinted under amphibolite facies conditions. A concordant U–Pb age of 316±1 Ma obtained from magmatic titanite of the posttectonic Verkniy Ufaley intrusion (Fig. 1b) dates the crystallization of this intrusion and provides a minimum age for the subduction and subsequent amphibolite facies overprint of the continental margin (Hetzel and Romer 1999).

In the central and southern part of the Sysert-Ilmenogorsk complex a nepheline-syenite intrusion extends for ~100 km NNE–SSW (Fig. 1b). The northern part of the syenite is called the Vishnevogorsk complex, whereas the southern part is referred to as the Ilmenogorsk complex (Levin 1974). The crystallization age of the syenite is considered to be Ordovician/Lower Silurian, based on two Rb–Sr whole-rock ages of 446±13 and 478±55 Ma, and a U–Pb zircon age of 434+ 15/–10 Ma (Kramm et al. 1983, 1993); thus, the intrusion predates the Uralian orogenic evolution and is probably related to the rifting of the Uralian paleoocean in the Ordovician (Kramm et al. 1983; Puchkov 1997).

Geochronological data from the Ufaley complex and the Sysert-Ilmenogorsk complex indicate markedly different metamorphic histories west and east of the Main Uralian fault. K–Ar and Ar–Ar mica ages from the East Ufaley complex range from 290 to 320 Ma (Lennykh 1963; Eide et al. 1997; Glasmacher et al. 1999); an additional Ar–Ar amphibole age is 308±3 Ma (Glasmacher et al. 1999). These ages have been interpreted to date the cooling below 300–350 °C at ~300 Ma. Isotopic ages suggest that the Sysert-Ilmenogorsk complex cooled through this temperature interval approximately 30–60 Ma later. K–Ar mica and feldspar ages fall mainly in the time interval between 270 and 240 Ma (Echtler et al. 1997) and three Rb–Sr mineral isochrons from the nepheline-syenite intrusion yield ages of 244±5, 245±24, and 244±8 Ma (Kramm et al. 1983).

The Kyshtym shear zone

General features

The nepheline-syenite intrusion and adjacent gneisses and amphibolites of the Sysert-Ilmenogorsk complex are transected by a several-kilometre-wide ductile shear zone, herein referred to as the Kyshtym shear zone (termed after the town Kyshtym; Fig. 2). Subsequently, a brittle fault, oriented subparallel to the shear zone, caused an additional displacement of several kilometres (Fig. 2). Exposure of rock in this area is, in general, poor and often restricted to road cuts. Our study focused on the central sector of the shear zone, approximately 20 km SW of Kyshtym, where recent excavations along a small road offered locally good exposure (Fig. 3). Exposed rock-types include biotite-rich metagranitoid, amphibolite, and, close to the Main Uralian fault, locally marble and ultramafic rocks. No nepheline syenite has been found, although its presence in the shear zone is well documented (e.g., Ronenson 1966; Levin 1974). Except for ultramafic low-strain lenses, all lithologies are strongly deformed as evident from the subvertical ~N/S-striking mylonitic foliation and a subhorizontal stretching lineation (Fig. 4).

Microstructural evolution

The deformation fabrics of feldspar and quartz combined with either the syntectonic recrystallization and growth or the retrograde transformation of minerals, such as pyroxene, amphibole, and biotite, indicate lower amphibolite to middle/lower greenschist facies conditions during the activity of the Kyshtym shear zone. In thin section, relic domains characterized by high-temperature deformation fabrics are visible in rocks affected by deformation under lower-grade conditions. This observation and the lack of microstructures characteristic for recovery processes indicate decreasing temperature during ductile deformation. The microstructural evolution is outlined herein beginning with the description of fabrics that developed under relatively high-temperature conditions followed by those formed at lower temperature.

Highly strained amphibolite exhibits alternating layers of green amphibole and recrystallized plagioclase. Amphibole has a strong shape-preferred orientation, whereas plagioclase subgrains show pronounced undulatory extinction. Locally, amphibolites contain relics of stretched clinopyroxene phenocrysts which were transformed to green amphibole at their margins. Retrogression of pyroxene is most pronounced along shear bands which are associated with

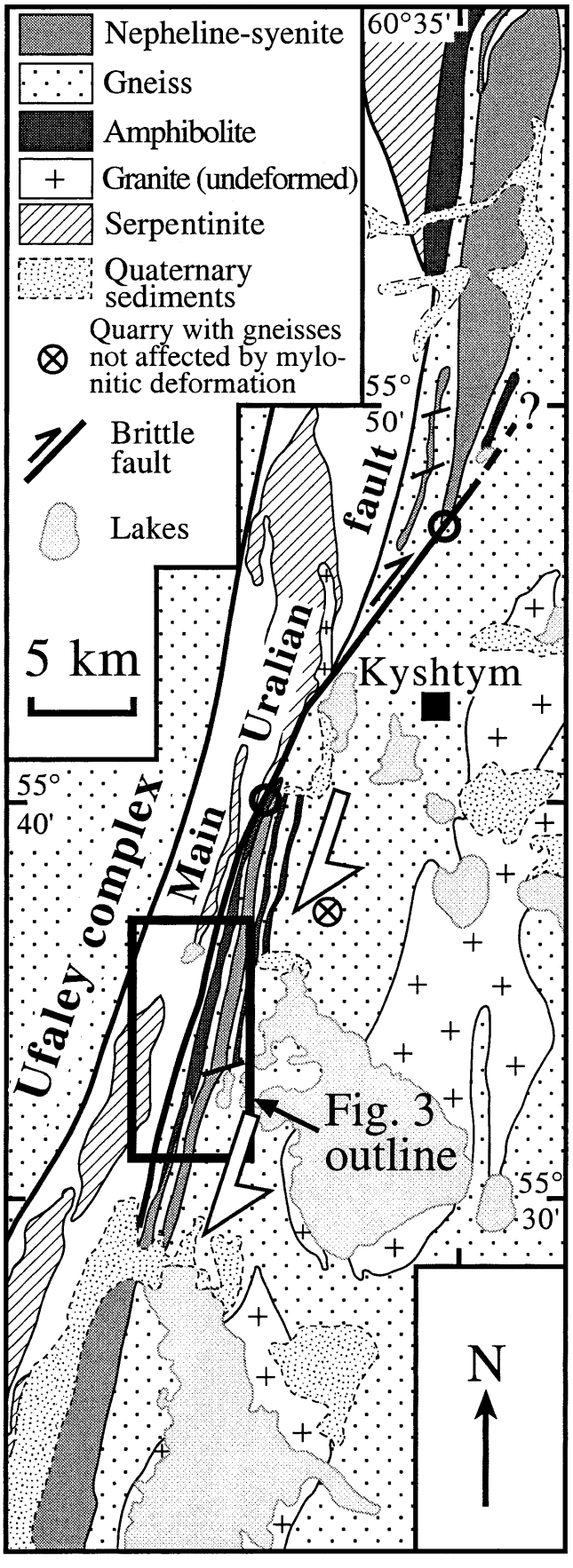

Fig. 2 Geological map showing the dextral ductile shear zone (*two white arrows*) transecting the central part of the Sysert-Ilmenogorsk complex. The left margins of the two arrows define the assumed eastern shear zone boundary. Map is based on the Russian 1:200,000 geological map N-41-I (Kyshtym) published in 1967. The *two circles* at the terminations of the ductily deformed syenite bodies indicate a displacement of 15 km along the brittle fault. Location of map area is shown in Fig. 1

newly formed, fine-grained green amphibole. Breakdown of pyroxene, syntectonic growth of amphibole, and complete recrystallization of plagioclase indicate lower amphibolite facies metamorphic conditions during ductile deformation.

Intensely deformed biotite-bearing granitoids, further referred to as quartz-feldspar mylonites, constitute the most abundant rock type in the area. Locally, the syntectonic recrystallization of feldspar in these rocks has gone to completion (Fig. 5a). However, most quartz-feldspar mylonites contain some feldspars that show core-and-mantle structures, i.e., rigid feldspar grains mantled by smaller feldspar (cf. Pryer 1993). Grain-size reduction of feldspar during dynamic recrystallization is interpreted to have occurred by subgrain rotation and the nucleation of new grains. Quartz exhibits undulatory extinction, serrated grain boundaries, and nucleation and growth of new grains, all indicative of dislocation creep during recrystallization (Fig. 5b). Feldspar and quartz fabrics are typical of lower amphibolite/upper greenschist facies conditions (Passchier and Trouw 1996). Such metamorphic conditions are also inferred by the presence of syntectonic muscovite (Fig. 5b) and biotite along shear planes and the marginal retrogression of rare amphibole to biotite.

Other mylonites show predominantly brittle deformation features in feldspar such as kink bands and shear fractures which occasionally acted as nucleation sites for small feldspar grains. Quartz in these rocks is deformed into extremely elongate grains that have aspect ratios of up to 10 and a width of 10–30 μm. Biotite is completely recrystallized and partially transformed to fine-grained chlorite. Taken together these observations suggest middle to lower greenschist facies conditions, although at the thin-section scale few domains of higher-grade deformation fabrics are locally preserved.

In summary, the microstructures indicate that the mylonites within the Kyshtym shear zone formed at retrograde lower amphibolite to middle/lower greenschist facies metamorphic conditions, i.e., at temperatures decreasing from approximately 550 °C to approximately 350 °C during deformation. Abundant kinematic indicators (cf. Passchier and Trouw 1996) record a consistent dextral shear sense for the mylonites and include quartz oblique grain shape fabrics (Fig. 5b), mica fish (Fig. 5c), σ-clasts, and extensional shear bands in both amphibolites and quartz-feldspar mylonites (Fig. 5d).

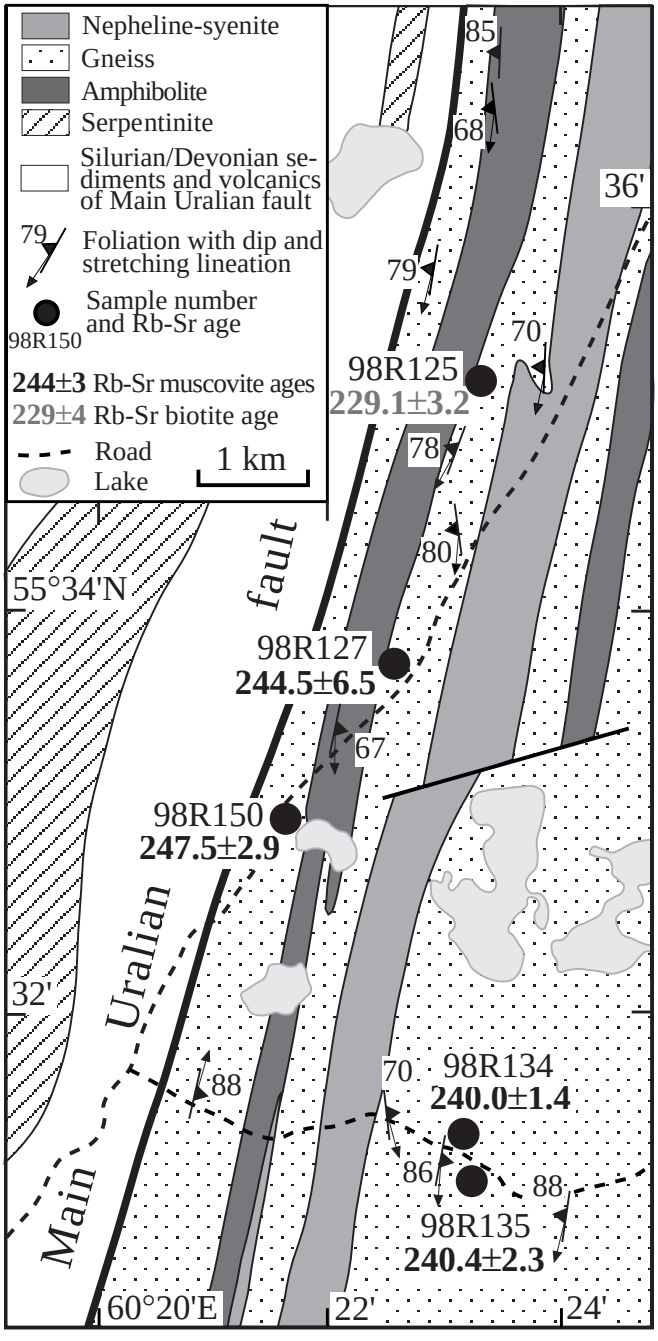

Fig. 3 Geological map of the central part of the Kyshtym shear zone with position of the five samples used for Rb–Sr analysis. Location of map area is shown in Fig. 2

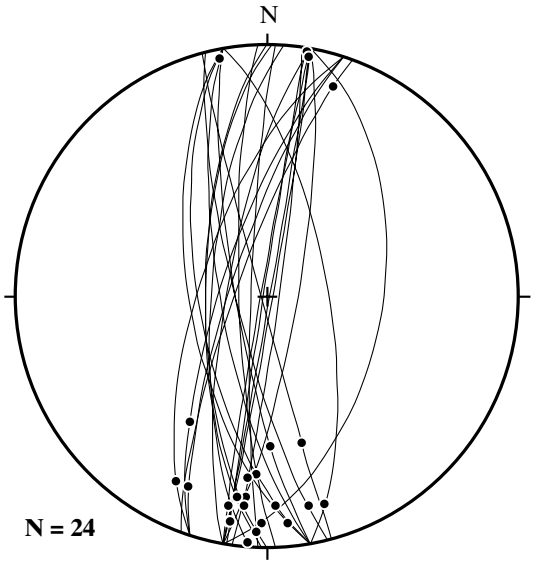

Fig. 4 Mylonitic foliation (*great circles*) and stretching lineations (*dots*) from the Kyshtym shear zone. Lower hemisphere equal-area projection

Rb–Sr dating

Deformation-induced resetting of the Rb/Sr system: sampling strategy

When dating the time of deformation in mylonites using isochron methods such as Rb/Sr the following important criteria must be met:

1. Initial isotopic equilibrium among two or more reservoirs in the mylonite is a prerequisite for dating mylonites. Such reservoirs may be separate mineral phases, but also individual crystals or small portions of whole rock. During progressive ductile deformation and dynamic recrystallization, fast diffusion pathways, such as dislocations and migrating grain boundaries, are abundant. So it is likely that during mylonitization isotopic equilibrium will be achieved on a local, maybe centimeter scale among all contemporaneously neo/recrystallizing minerals.
2. Textural equilibrium is a prerequisite for isotopic equilibrium. Mineral grains forming relictic porphyroclasts have obviously not recrystallized during the deformation event to be dated. Therefore, these minerals can be expected to be isotopically out of equilibrium with their environment as well. Utmost care must be taken to avoid such relics in the sampling and mineral preparation process. Consequently, mylonites showing abundant feldspar porphyroclasts ("augen") should be dismissed.
3. The third important aspect for dating is that the equilibria once adjusted during mylonitization must be preserved since the time of mylonitization; thus, the metamorphic temperature after ductile deformation must remain below the lower temperature limit for thermally induced reopening of the Rb/Sr systems (e.g., Freeman et al. 1997). In addition, late-stage processes, such as diaphthoritic alteration or weathering, may disturb the isotopic signatures of specific minerals. In particular, biotite and, to a lesser degree, feldspar are affected by such processes. As a result, fresh samples are favorable for analysis.

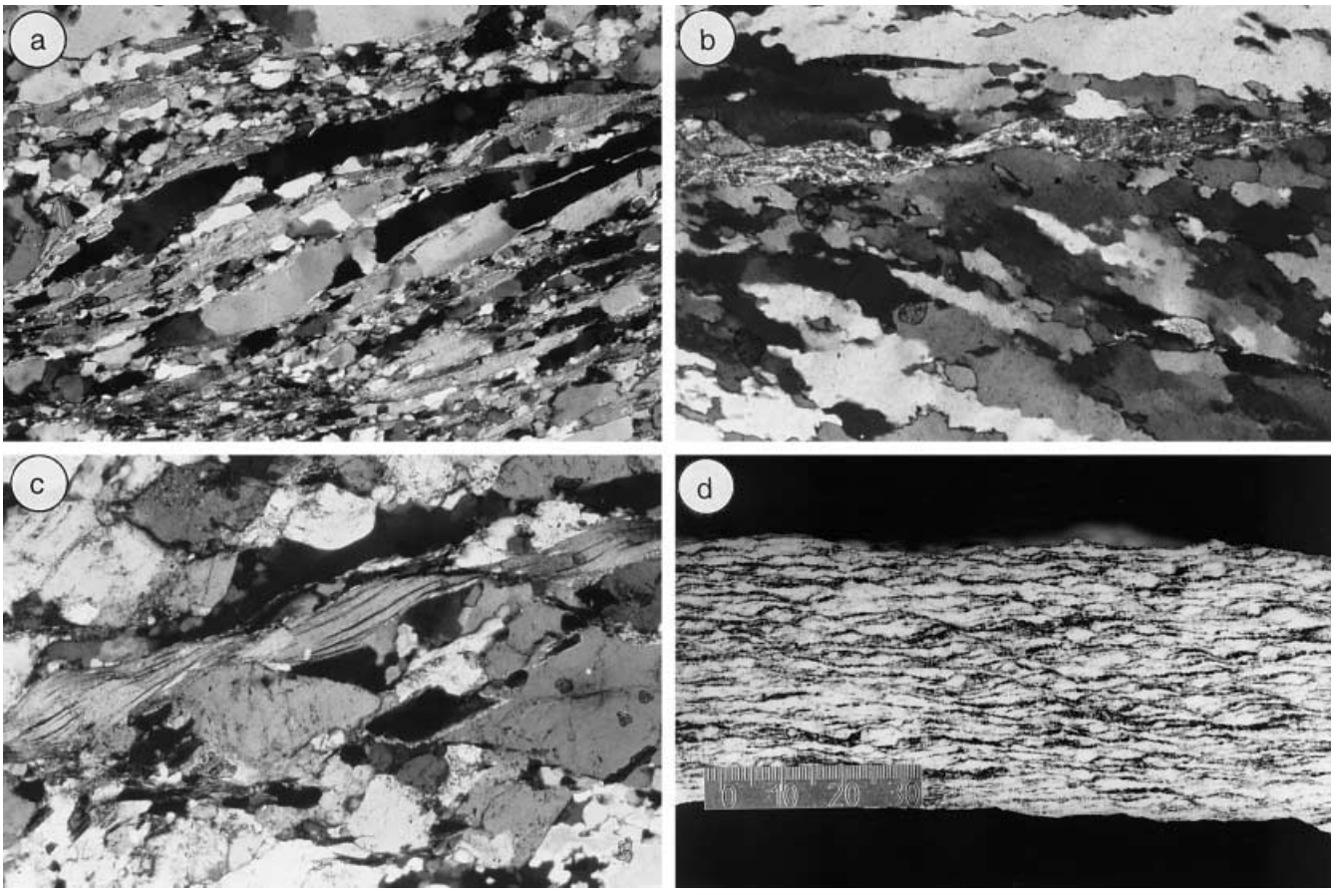

Fig. 5a–d Lower amphibolite/upper greenschist facies mylonites from the Kyshtym shear zone, Middle Urals, Russia. The photomicrographs shown in **a–c** are from samples 98R150, 98R134, and 98R127, which were used for Rb–Sr analysis. **a** Mylonite (98R150) showing complete recrystallization of feldspar (small grains) and quartz (large, elongated grains). Note abundant syntectonic muscovite flakes that define the foliation. Width of photomicrograph is 2.5 mm. Crossed nicols. **b** Recrystallized quartz layer in mylonite (98R134). Quartz shows undulose extinction, serrated grain boundaries, and growth of small, new grains. The main foliation is horizontal and defined by a layer of syntectonic muscovite and elongated quartz grains in the upper half of the picture. In the lower half of the picture, an oblique quartz grain shape fabric, defined by the long axes of quartz grains, indicates a sinistral sense of shear (=dextral in nature). Width of photomicrograph is 1 mm. Crossed nicols. **c** Three deformed muscovite grains in a matrix of recrystallized feldspar and minor amounts of fine-grained quartz (98R127). The three mica fish indicate a dextral shear sense. The long axes of the muscovite fish are ~600 μm long. See text for further explanation. Width of photomicrograph is 2 mm. Crossed nicols. **d** Biotite-rich quartz-feldspar mylonite. The main foliation is parallel to the long side of photomicrograph. Numerous extensional shear bands indicate a dextral sense of shear. *Scale bar* is 30 mm

In order to determine the age of the Kyshtym shear zone, five mylonites (98R125, –127, –134, –135, –150) were selected for Rb–Sr analysis after careful inspection under the optical microscope. The samples are meta-granitic in composition and show mylonitic textures. The main phases are plagioclase, K-feldspar, quartz, ±muscovite, ±biotite/chlorite, ±garnet, apatite, and zircon. In most samples indications for a slight diaphthoritic overprint, such as local chloritization of biotite and sericitization of feldspar, are present. The rocks were mylonitized at lower amphibolite/upper greenschist facies conditions as indicated by the dynamic recrystallization of feldspar and the syntectonic stability and/or growth of muscovite and biotite. From microtextural observations minerals for which complete syndeformational equilibration can be inferred are biotite, muscovite, quartz, and feldspar. However, in sample 98R134 and possibly in sample 98R127, small amounts of feldspar relics are locally present. For apatite it is difficult to assess from microtextural observations alone whether it recrystallized during deformation. For dating the deformational event, we prepared whole-rock powder and mineral separates of muscovite, biotite/chlorite, and feldspar from small, lithologically homogeneous samples of approximately 100 g: The smaller the sample is, the more likely it is that isotopic rehomogenization during deformation was effective on a scale exceeding the sample size. Apatite was separated and analyzed as well in order to test its behavior in the mylonitization process. In addition, we preferred muscovite-bearing samples since muscovite is more resistant than biotite with respect to diaphthoritic alteration.

Analytical procedures

For the Rb–Sr isotope analyses, mineral concentrates of muscovite, biotite, apatite, and feldspar were produced. Great care was taken to avoid material altered by weathering. Mica concentrates were ground under pure ethanol in a polished agate mortar and then sieved in ethanol in order to obtain clean, inclusion-free mica separates. The concentrates were finally purified by hand-picking under the binocular microscope. Whole-rock powders were prepared in an agate mill. Samples were analyzed for Rb and Sr contents by isotope dilution. They were weighted into Savillex screw-top containers, spiked with suitable mixed ^{87}Rb-^{84}Sr spike solutions, and dissolved in a mixture of HF and HNO_3. Solutions were processed by standard cation-exchange techniques. Determinations of Sr isotope ratios were carried out on a VG Sector 54 multicollector thermal ionization mass spectrometer (GeoForschungsZentrum, Potsdam, Germany) in dynamic mode. The value obtained for ^{87}Sr/^{86}Sr of the NBS standard SRM 987 during the period of analytical work was 0.710263±0.000010 (n=16). All isotopic ratios were normalized to an ^{86}Sr/^{88}Sr ratio of 0.1194. Rb analyses were done on a VG Isomass 54 single collector TIMS instrument. The observed ratios were corrected for 0.25% per a.m.u. mass fractionation. Total procedural blanks were consistently below 0.10 ng for both Rb and Sr. Due to small and highly variable blank values, a useful blank correction is not applicable. For age calculations, an uncertainty of ±1%, as derived from replicate analyses of natural mica samples, is assigned to the ^{87}Rb/^{86}Sr ratios. ^{87}Sr/^{86}Sr ratios are reported with their 2-σ internal precision plus uncertainties from spike correction. In the calculations of isochron parameters, a standard error of ±0.005% for ^{87}Sr/^{86}Sr ratios was applied if individual errors were smaller than this value. This error estimate (2 σ) was derived from reproducibility tests for Sr isotope ratios of spiked samples. Regression lines are calculated using Isoplot/Ex 2.06 (Ludwig 1999). A decay constant for Rb of 1.42×10^{-11} a^{-1} (Neumann and Huster 1974) was used for all age calculations.

Analytical results

The Rb–Sr data are summarized in Table 1 and illustrated in Fig. 6. Sample 98R150 yields an isochron age of 247.5±2.9 Ma, defined by two sieve fractions of muscovite (100–160 and 355–500 μm), plagioclase, apatite, and the whole-rock data (Fig. 6a). Syntectonic

Table 1 Rb–Sr data from the Kyshtym shear zone, middle Urals, Russia

	Rb (ppm)	Sr (ppm)	^{87}Rb/^{86}Sr	^{87}Sr/^{86}Sr	^{87}Sr/^{86}Sr 2 σ (%)
Sample 98R150: **247.5±2.9 Ma**					
Apatite	4.11	3413	0.003	0.704884	0.0020
Feldspar (>250 μm)	27.79	1513	0.053	0.705024	0.0051
Whole rock	69.57	1167	0.172	0.705489	0.0016
Muscovite (100–160 μm)	393.4	137.5	8.297	0.733924	0.0016
Muscovite (355–500 μm)	413.7	116.4	10.32	0.741367	0.0022
Sample 98R127: **244.5±6.5 Ma**					
Apatite	0.75	387.6	0.006	0.703989	0.0016
Plagioclase (>250 μm)	4.80	874.2	0.016	0.703989	0.0016
Whole rock	27.37	548.3	0.144	0.704291	0.0014
Muscovite (<125 μm)	151.1	40.95	10.71	0.740625	0.0018
Muscovite (355–500 μm)	169.7	37.35	13.20	0.750215	0.0020
Biotite (<500 μm)[a]	528.5	19.08	81.19	0.838836	0.0021
Sample 98R134: **240.0±1.4 Ma**					
Apatite	13.11	116.2	0.327	0.713760	0.0027
Feldspar (>250 μm)[a]	77.01	146.4	1.523	0.717319	0.0015
Whole rock	146.4	132.3	3.207	0.723607	0.0022
Muscovite (125–160 μm)	430.3	12.23	105.4	1.071020	0.0014
Muscovite (355–500 μm)	467.6	10.61	133.3	1.169098	0.0014
Biotite (<500 μm)[a]	920.4	7.50	399.3	1.983834	0.0010
Sample 98R135: **240.4±2.3 Ma**					
Apatite	3.54	378.8	0.027	0.705396	0.0016
Feldspar	96.15	584.8	0.476	0.706909	0.0016
Whole rock	93.03	521.3	0.516	0.707044	0.0016
Muscovite (80–100 μm)	281.4	51.36	15.93	0.759872	0.0014
Sample 98R125: **229.1±3.2 Ma**					
Plagioclase (>250 μm)	7.44	963.0	0.022	0.703955	0.0016
Apatite	2.67	262.0	0.029	0.703963	0.0024
Whole rock	24.13	690.9	0.101	0.704226	0.0016
Biotite (<250 μm)	278.8	14.61	56.19	0.888472	0.0016
Biotite (250–355 μm)	305.0	8.79	103.6	1.039585	0.0016

[a] Mineral excluded from age calculation. See text for further details

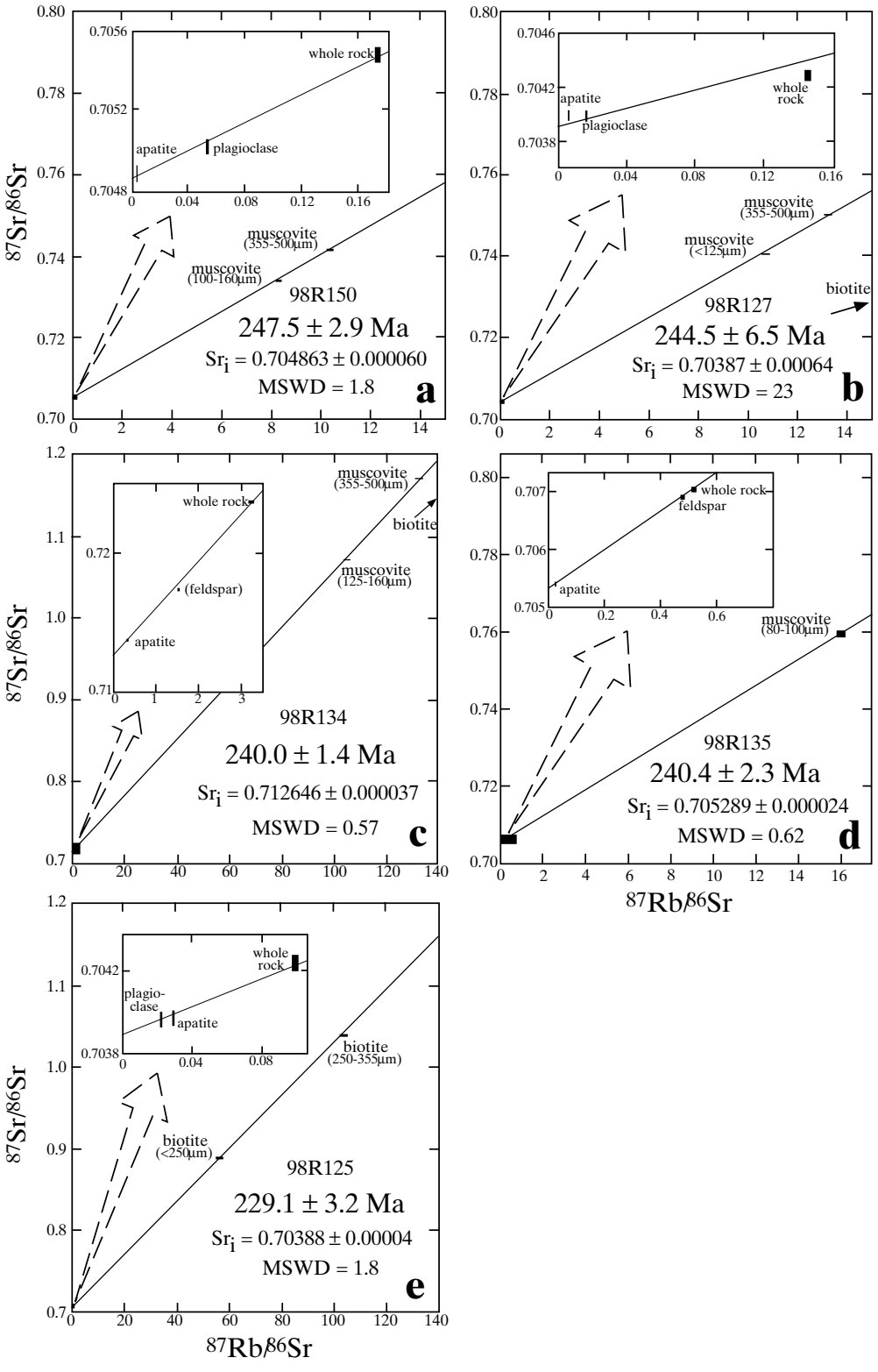

Fig. 6a–e Rb–Sr isochron diagrams of five mylonites from the Kyshtym shear zone. Sample locations are shown in Fig. 3

biotite is extremely finegrained in this sample and has not been separated. Sample 98R127 yields mineral data which do not fit on a single isochron. If the two muscovite sieve fractions (<125 and 355–500 μm), apatite, plagioclase, and the whole-rock data are used for regression calculation, the slope of the regression line corresponds to an age of 244.5±6.5 Ma (MSWD=23; Fig. 6b). When the two muscovite fractions of 98R127 are combined separately with the plagioclase data, two slightly different apparent ages are obtained. The coarse-grained muscovite yields an age value of 246.5± 2.4 Ma, whereas the fine-grained muscovite has an

apparent age of 240.8±2.4 Ma. Biotite/chlorite in 98R127 plots far below the regression line defined by the other mineral data. The whole rock–biotite/chlorite apparent age is 116.8±1.1 Ma. Sample 98R134 gives an isochron age of 240.0±1.4 Ma based on two muscovite fractions (125–160 and 355–500 μm), apatite, and the whole-rock data (Fig. 6c). Feldspar and biotite/chlorite plot slightly below the isochron and have not been included in the regression analysis. If combined with apatite, biotite/chlorite gives an apparent age of 223.8±2.2 Ma. 98R135 yields an isochron age of 240.4±2.3 Ma based on one muscovite fraction (80–100 μm), feldspar, apatite, and the whole-rock data (Fig. 6d). Sample 98R125, which does not contain any muscovite, yields an isochron age of 229.1± 3.2 Ma, defined by two grain-size fractions of biotite/chlorite (<250 and 250–355 μm), plagioclase, apatite, and the whole-rock data (Fig. 6e).

Estimate of displacement magnitude for the Kyshtym fault system

Assuming a simple initial shape for the nepheline syenite body, we use a simple two-stage model to reproduce its deformed shape and the present orientation of the tectonic foliation in the Kyshtym shear zone (Fig. 4). During the first stage, the fault system evolves by ductile shearing, whereas the second stage is characterized by brittle faulting (Fig. 7). The present width of the syenite body in its northern part (Vishnevogorsk complex), not affected by the shear zone, is 3.5 km (Fig. 2). The width of the southern part (Ilmenogorsk complex) varies between 2 and 4 km. The nepheline syenite intrusion may have had an elongate shape, due to intrusion along a fault system related to rifting and passive margin development. In our model a rectangle 3.5 km in width represents the initial shape of the syenite body (Fig. 7a). As the

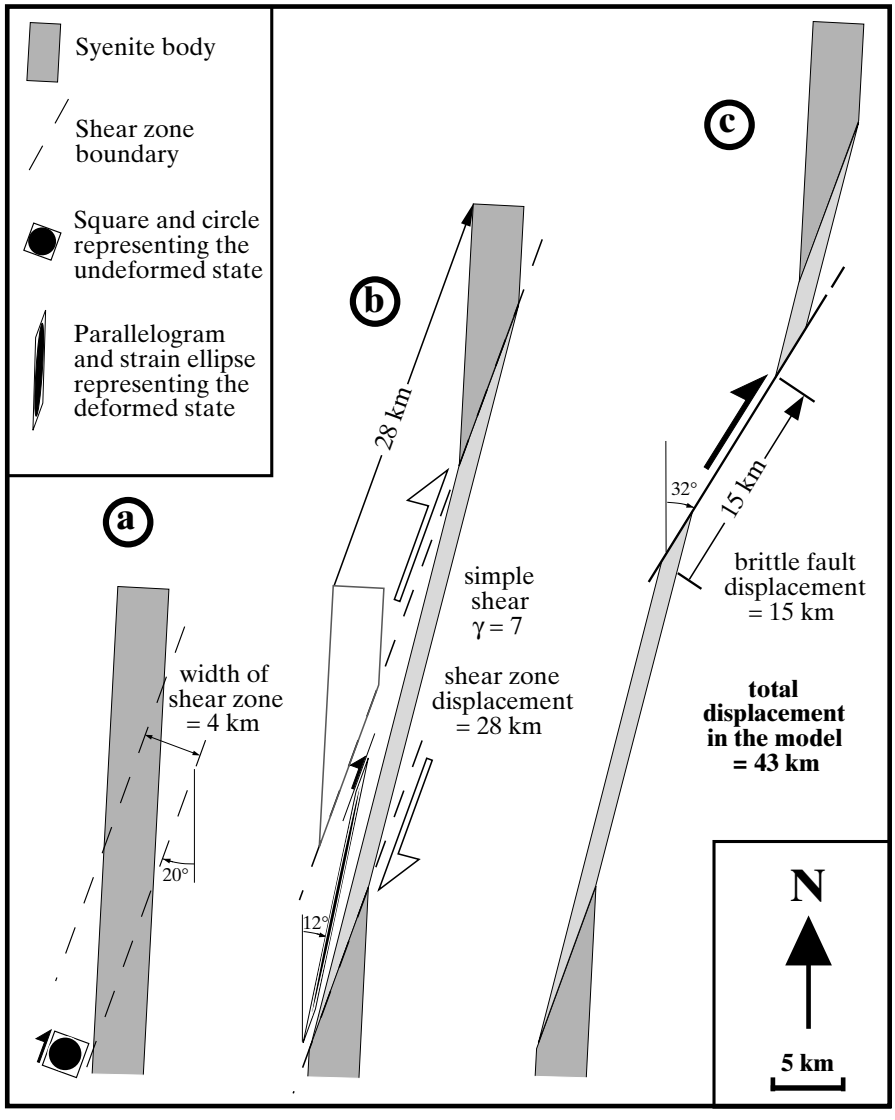

Fig. 7a–c Two-stage model for the evolution of the dextral Kyshtym fault system. **a** Simplified geometry of the syenite before ductile shearing. Shear zone is 4 km thick and shear zone boundaries are oriented N20°E. Width of the syenite is 3.5 km. **b** Geometry of the syenite after a dextral simple shear (shear strain γ=7). Displacement is 28 km. X-axis of finite strain ellipse shown in black is oriented N12°E. **c** Geometry after 15 km of displacement along the N32°E trending brittle fault. Compare final geometry with map shown in Fig. 2. See text for further discussion

boundaries of the Kyshtym shear zone are not exposed, the orientation of the shear zone boundaries in the model is taken to be N20°E (Fig. 7a), i.e., parallel to the southeastern margin of the Ufaley complex (Fig. 2). The minimum thickness of the shear zone is 4 km, as observed along a road oriented perpendicular to the shear zone in the southern part of Fig. 3. A maximum thickness of 5 km is given by the observation that upper amphibolite facies gneisses exposed in a quarry located 5 km east of the Main Uralian fault (55°37.7'N; 60°30.0'E; see Fig. 2) do not show any mylonitic fabrics.

If the walls of a shear zone remain undeformed and no volume change occurs, the shear zone must form by simple shear (Ramsay and Graham 1970). The following arguments suggest that during formation of the Kyshtym shear zone no significant deformation of the wall rocks has occurred; thus, in our model the first stage of ductile shearing is approximated by simple shear (Fig. 7b). The gneisses in the quarry located east of the shear zone do not show any evidence of a mylonitic deformation indicating that the eastern shear zone wall remained undeformed. As outlined previously, the Ufaley complex situated west of the shear zone cooled below 300–350 °C tens of million years before the Sysert-Ilmenogorsk complex. This explains why the Ufaley complex behaved as a rigid block during the formation of the Kyshtym shear zone. As all lithologies within the Kyshtym shear zone have a well-developed mylonitic foliation and a stretching lineation (except for minor ultramafic bodies), deformation in our model is homogeneous.

Ductile shearing has resulted in the pronounced NNE-directed stretching of the syenite and the amphibolite bodies (Fig. 2). The length/width ratios of these bodies in map view, as obtained from the Russian 1:200,000 geological map, is used to estimate the amount of shear. The length/width ratio of the three amphibolite bodies in the central part of the shear zone is ~30, ~60, and ~80; the elongate syenite body between these amphibolites has a length/width ratio of ~40 (Fig. 2). A strain ellipse will have a ratio of the principle strain axes (X/Z) between ~30 and ~80 if the shear strain γ is between 5 and 9 [Eqs. (3–67) in Ramsay 1967]. In our model, we adopt a more conservative range of shear strain between 4 and 10, i.e., γ=7±3 to account for the uncertainty of the length/width ratios measurements. As the undeformed bodies were probably not circular in map view but had an elongate shape with a long axis oriented ~N–S, the amount of shear is a maximum estimate. A shear strain of γ=7±3 results in a displacement magnitude of 28±12 km assuming homogeneous simple shear (Fig. 7b). For a shear strain of γ=7 the angle between the X-axis of the finite strain ellipsoid and the shear zone boundary is 8° [Eq. (36) in Ramsay and Graham 1970]. With the shear zone boundaries oriented N20°E, this results in a N12°E orientation of the long axis of the finite strain ellipsoid (Fig. 7b). This is in good agreement with the orientation of the highly stretched syenite and amphibolite bodies and the strike of the mylonitic foliation in the Kyshtym shear zone (Figs. 3, 4).

A dextral brittle fault trending N32°E transects the ductily deformed syenite and caused an additional displacement during the second stage of deformation (Fig. 7c). Restoration of the ductily thinned terminations of the displaced syenite bodies indicates that the offset along the brittle fault is 15±3 km (indicated by two circles in Fig. 2). The error of three kilometers is estimated from the good fit of the displaced bodies in map view; thus, the total displacement for the Kyshtym fault system is 28±12+15±3 km=43±15 km. The model is in good agreement with all available geological observations.

Discussion

Deformation ages vs cooling ages

During the past decades isotopic data obtained by Rb–Sr mineral or Ar–Ar analyses of metamorphic rocks have widely been interpreted as cooling ages in terms of the closure temperature concept (Dodson 1973), i.e., the ages were thought to record the time when a sample cooled through a certain temperature. Based on several field studies, closure temperatures for the diffusion of Sr and Ar in white mica are assumed to be in the range of 550±50 °C and 350±50 °C, respectively, whereas the closure temperature for Sr diffusion in biotite is estimated at 350±50 °C (Jäger 1973; von Blanckenburg et al. 1989, and references therein; Hames and Bowring 1994). In general, the closure-temperature concept has been used regardless of the deformation history of the sample. However, it has recently been shown that deformation may be far more efficient in resetting the Rb–Sr and K–Ar isotope systems than temperature (Freeman et al. 1997; Dunlap 1997; Villa 1998; Müller et al. 1999). For interpreting isotope data from mylonites it is thus of crucial importance to know whether the metamorphic conditions during ductile deformation were above or below the closure temperature with respect to the isotope system of interest (Freeman et al. 1997; Dunlap 1997; Reddy and Potts 1999). Deformation events can only be constrained if the temperatures during deformation were below the closure temperature of a particular isotope system; otherwise, isotopic ages may be cooling ages. We emphasize that for samples which escaped deformation and fluid rock interaction during their retrograde metamorphic evolution the commonly accepted closure-temperature estimates might be too low (Villa 1998).

As pointed out previously, the microstructural evolution recorded by the mylonites from the Kyshtym shear zone indicates that metamorphic conditions during ductile deformation decreased from lower amphibolite facies to middle/lower greenschist facies con-

ditions, i.e., from ~550 to ~350 °C. For the Rb–Sr study, mylonites that were deformed in the upper temperature range (i.e., 550–450 °C) were chosen, as in such samples feldspar and apatite have most likely isotopically equilibrated with mica. Samples that were deformed in the lower temperature range (i.e., ~350–450 °C), as indicated by the brittle deformation of feldspar, were avoided since for such samples the presence of textural disequilibria implies isotopic disequilibria.

Sample 98R150 (247.5±2.9 Ma) records a perfect syndeformational Sr-isotopic reequilibration between muscovite, plagioclase, and apatite. Two grain-size fractions of muscovite fall on the same isochron indicating an isotopically homogeneous muscovite population with respect to Sr, i.e., the absence of any muscovite relics predating ductile deformation (see Fig. 5a). Sample 98R127 yielded data which do not define a single isochron age but indicate the presence of grains (muscovite and possibly feldspar) that form relics with respect to the last stage of deformation. The result of a linear regression (244.5±6.5 Ma, MSWD=23) is interpreted as a "mixed age," averaging a prolonged process of syndeformational recrystallization. The fact that two different grain-size fractions of muscovite give slightly different apparent ages when combined with the plagioclase data (i.e., 246.5±2.4 and 240.8± 2.4 Ma) suggests that during progressive deformation the deformation-induced isotopic resetting has ceased earlier in the larger grains than in the smaller ones. This interpretation is justified by the fact that ongoing deformation at falling temperatures caused grain-size reduction, leaving "big" muscovites as relics from earlier stages of ductile deformation. Such relatively big muscovites are shown in Fig. 5c. It is highly unlikely that the grain-size dependence of apparent ages is caused by thermally driven diffusional processes alone: It has been shown recently that, in absence of crystal-plastic deformation, Sr isotope exchange between mica and other phases may be kinetically inhibited up to temperatures well above the commonly assumed closure temperatures (Kühn et al. 2000). Biotite/chlorite from 98R127 yields an anomalously young apparent age of 116.8±1.1 Ma, when combined with the whole-rock data. This apparent age is interpreted to result from the removal of radiogenic Sr from biotite by retrogressive fluids during partial chloritization. Since the biotite/chlorite mineral separate is a mixture of different phases related to different stages of the petrologic evolution, the apparent age of 116.8±1.1 Ma has no direct geological meaning. However, the data constrain the age of the retrogression event(s) to be Cretaceous or younger. A net removal of radiogenic Sr from the biotite and the whole-rock by retrogressive fluids also explains the small downward shift of the whole-rock data point relative to apatite and plagioclase (Fig. 6b). Sample 98R134, with an isochron age of 240.0±1.4 Ma, contains small amounts of feldspar relics. This explains that the data point for feldspar (grain size of >250 μm) plots slightly below the isochron (the average grain size of feldspar in the sample is smaller). Biotite/chlorite of this sample gives an age value of 223.8±2.2 Ma when combined with apatite, an apparent age that is considerably younger than that of muscovite. Sample 98R135 (240.4± 2.3 Ma) records a perfect syndeformational Sr-isotopic reequilibration between muscovite, feldspar, and apatite. Sample 98R125, which does not contain any muscovite, yields an apparently well-constrained isochron age of 229.1±3.2 Ma. Two grain-size fractions of biotite/chlorite lie on the same isochron indicating an isotopically homogeneous biotite/chlorite population with respect to Sr.

Since ductile deformation within the dated mylonites stopped at a temperature below the closure temperature for Sr diffusion in muscovite, i.e., 550±50 °C, the muscovite ages are interpreted as deformation ages. In other words the muscovite ages date the lower amphibolite/upper greenschist facies deformation recorded in the five mylonites. The difference in age between the oldest (247.5±2.9) and youngest age (240.0±1.4) suggests that the Kyshtym shear zone was active for several million years. This is supported by the different ages obtained from two muscovite grain-size fractions of 98R127 (246.5 and 240.8 Ma). The larger muscovite grains of 98R127 yield an age that is identical within error to that of 98R150, suggesting that these larger grains were isotopically equilibrated during an early stage of the deformation history; thus, it is extremely unlikely that the large grains from 98R127 predate the ductile shearing. The smaller muscovite grains of 98R127 yield an age that is identical within error to the muscovite age of samples 98R134 and 98R135.

The interpretation of the biotite/chlorite age values is less straightforward than that of the muscovite ages. In all samples, biotite is at least partly chloritized. Biotites affected by chloritization generally exchange their Sr with surrounding fluids to a greater or lesser extent, a process leading to anomalously young apparent biotite ages. Even minor, hardly detectable chloritization or weathering of biotite is known to "rejuvenate" apparent ages of biotite (Clauer et al. 1982). The age of the chloritization is Cretaceous or younger, as constrained by the youngest apparent age found for a biotite/chlorite mixture (116.8±1.1 Ma).

The geological meaning of the highest apparent biotite/chlorite age (229.1±3.2 Ma; sample 98R125) needs to be discussed in some detail. The following arguments suggest that the age of 229.1±3.2 Ma represents a minimum age for the deformation in the sample. During deformation, at temperatures above 350 °C, the Rb/Sr system of biotite was equilibrated with the matrix phases as biotite shows syntectonic recrystallization. After the end of deformation, biotite may or may not have remained as an open system for Rb/Sr. If the temperatures after the end of deformation were, for a certain period, high enough to

mediate isotope exchange, the data must be interpreted as a cooling age. However, it is known that in the absence of free fluids and deformation, Rb/Sr isotope exchange involving biotite may be kinetically inhibited up to temperatures far in excess of the commonly assumed closure temperature of 350 °C (Kühn et al. 2000). In that case the biotite age dates the end of deformation. Since a small degree of chloritization is present in the sample, and chloritization is known to "rejuvenate" biotite ages, we interpret the age value of 229.1±3.2 Ma as a minimum age either for deformation or for cooling below ca. 350 °C. In any case, crystal-plastic deformation ceased prior to 229.1± 3.2 Ma, and probably already at ca. 240 Ma, the time given by the youngest muscovite ages.

Kramm et al. (1983) report Rb–Sr mineral ages from samples of the Vishnevogorsk- and the Ilmenogorsk complexes that were collected from outside the Kyshtym shear zone. Their samples contained biotite, K-feldspar, whole rock, sphene, apatite, and cancrinite. Three mineral ages (mainly biotite-based) are 244±8 Ma, 244±5 Ma (Vishnevogorsk complex), and 245±24 Ma (Ilmenogorsk complex; Kramm et al. 1983). The age values obtained are, within limits of error, in perfect agreement with our age data from the Kyshtym shear zone. Kramm et al. (1983) have interpreted their mineral ages as "cooling ages after an amphibolite grade metamorphism." Taken together, the available age information demonstrates that the time interval 250–240 Ma was characterized by intense ductile shearing localized in the Kysthym shear zone, and coeval cooling of the Ilmenogorsk- and Vishnovogorsk syenite complexes after amphibolite facies metamorphism.

Duration of ductile deformation in the Kyshtym shear zone

We calculate a strain rate for the Kyshtym shear zone using our shear strain estimate and Rb–Sr muscovite age data. We emphasize that these calculations are only rough estimates due to the errors of both the shear strain estimate and the Rb–Sr ages. Nevertheless, it is possible to derive an approximate upper bound for the duration of ductile deformation in the Kyshtym shear zone. Natural strain rates have been estimated to range between 10^{-13} and 10^{-15} s^{-1} (Pfiffner and Ramsay 1982, and references therein). At a very low strain rate of 1×10^{-15} s^{-1}, it takes longer than 10 Ma to produce even a very small finite strain such as X/Z=2, a value which has been referred to as slaty cleavage "front" by Pfiffner and Ramsay (1982). Higher strain rates of up to 10^{-12} s^{-1} are likely to occur in shear zones (e.g., Twiss and Moores 1992).

Shear strain of the Kyshtym shear zone has been estimated at γ=7±3. Accumulating a shear strain of γ=7 in one million years translates into a strain rate of $\sim2\times10^{-13}$ s^{-1} (e.g., Twiss and Moores 1992). Such a rate seems to be in agreement with generally accepted values for strain rates in shear zones. It conflicts, however, with the geochronological results. The Rb–Sr muscovite ages suggest that ductile deformation under lower amphibolite/upper greenschist facies conditions was active for approximately 5–10 Ma, as the oldest and youngest muscovite ages are 247.5±2.9 and 240.0± 1.4 Ma, respectively. From the microstructural evolution it is conceivable that locally ductile deformation proceeded until temperatures decreased to middle/ lower greenschist facies conditions (i.e., ~350 °C); thus, deformation may have lasted longer than 5–10 Ma. The biotite/chlorite age of 229.1±3.2 Ma for sample 98R125 provides a minimum age estimate for the time at which ductile deformation had ceased. If our interpretation of this age is correct, ductile deformation has proceeded no longer than until ~230 Ma, but may have stopped as early as ~240 Ma. If the shear strain of γ=7 had accumulated in 20 Ma, i.e., between ~230 and 250 Ma, the strain rate would be $\sim1\times10^{-14}$ s^{-1}. As this is a small rate, compared with the strain rates compiled by Pfiffner and Ramsay (1982), we consider 20 Ma as a maximum for the activity of the Kyshtym shear zone. This is supported by slip rates obtained for active continental strike-slip faults, which range from several centimeters down to a few millimeters per year (e.g., Sieh and Jahns 1984; Peltzer et al. 1988; Meyer et al. 1996), assuming that the displacement of 28±12 km for the Kyshtym shear zone accumulated in 20 Ma results in a slip rate of 1.4±0.6 mm/year, which is in the lowermost range of slip rates derived from active continental strike-slip faults.

Transition from ductile to brittle deformation

Ductile deformation in the Kyshtym shear zone presumably ceased as the temperature decreased below ~300 °C, i.e., the temperature at which the transition from ductile to brittle deformation occurs in quartz-bearing crustal rocks (e.g., Stöckhert et al. 1999). Ductile deformation was followed by the formation of the dextral strike-slip fault which is oriented subparallel to the Kyshtym shear zone (Fig. 2). In other words, we interpret the brittle strike-slip fault to have initiated as a result of cooling of the internal parts of the Middle Urals during ongoing transcurrent movements. The slightly different orientation between the ductile shear zone and the brittle fault does not imply any change in the kinematics of the fault system. In the model (Fig. 7), the difference between the orientation of the ductile shear zone (N20°E) and the brittle fault (N32°E) is 12°. This small difference is explained by a different orientation of the failure plane for ductile and brittle deformation with respect to the maximum principal stress σ_1. In general, the angle between σ_1 and a ductile shear zone is assumed to be approximately 45°, i.e., shear zones form along the plane of maximum shear stress, whereas for brittle deformation

the angle between σ_1 and a shear fracture is approximately 30° (Twiss and Moores 1992, pp 142 and 171).

Implications of the Kyshtym fault system for the geodynamic evolution of the Urals

Regional strain patterns in continental collision zones have often been explored in terms of indentation models, i.e., models in which a rigid plate or block is driven horizontally into a mechanically weaker medium, causing widespread deformation in front of the block (e.g., Tapponnier and Molnar 1976; Peltzer and Tapponnier 1988; Huchon et al. 1994). In general, indentation starts with thrust faulting close to the indenter, as σ_1 (the maximum principal stress) is horizontal and σ_3 (the minimum principal stress) is oriented vertical. Thrust faulting and crustal thickening result in surface uplift and increase the vertical principal stress in the crust. Eventually, σ_2 will become the vertical principal stress and at this stage deformation will proceed through strike-slip faulting (Tapponnier and Molnar 1976). Strike-slip faults may accommodate the lateral displacement of material away from a collision zone (e.g., Dewey et al. 1986; Ratschbacher et al. 1991), a process which has been referred to as "extrusion tectonics" (Tapponnier et al. 1982) or "tectonic escape" (Burke and Sengör 1986).

The curvature of the Main Uralian fault in the Middle Urals reflects the shape of a promontory belonging to the East European craton (Fig. 1a; Puchkov 1997). The Ufaley complex forms the eastern part of this promontory and represents a part of the subducted East European continental margin (Echtler et al. 1997; Hetzel and Romer 1999). According to Echtler et al. (1997), the Ufaley complex behaved as indenter and caused a greater magnitude of horizontal shortening and crustal thickening in the Middle Urals than in other parts of the Uralide orogen. We envision the Kyshtym strike-slip fault system to have formed after Permian thrusting and crustal thickening along the southeastern margin of the Ufaley indenter. As the Kyshtym fault system accommodated an orogen-parallel mass transfer away from the region that presumably experienced the maximum amount of shortening, it can be interpreted to reflect the "tectonic escape" of material away from the Ufaley indenter.

Given the right-lateral mass transfer along the southeastern margin of the Ufaley indenter, the question arises as to whether material has also been transferred along the northeastern margin of the indenter. In other words, are there any sinistral faults that reflect the transfer of material towards the northwest relative to the Ufaley indenter. Indeed, a system of ~NW-trending strike-slip faults has recently been described north of latitude 56° (Fig. 1b), based on reflection seismic, aeromagnetic, and geologic data (Ayarza et al. 2000). The sinistral strike-slip faults have been interpreted to rework the Main Uralian fault zone, i.e., the original arc-continent suture; however, the timing of this deformation phase is not well constrained. We suggest that sinistral strike-slip faulting along the Main Uralian fault (Ayarza et al. 2000) may have occurred contemporaneously with the activity of the Kyshtym fault system. This assumption can be tested by geochronological investigations such as those applied in the present study. If the two strike-slip faults have the same Late Permian/Early Triassic age, they can be interpreted as a conjugate set that formed during the final collisional stage of the Urals.

Conclusion

The consistency of mylonitization ages for the different samples confirms that lower amphibolite/upper greenschist facies mylonites can be successfully dated by internal Rb/Sr mineral isochrons. During mylonitization, isotopic equilibration among muscovite, feldspar, and whole rock was achieved when microtextural equilibration was apparent in thin section. The mineral data set demonstrates that the Sr in apatite was isotopically equilibrated with Sr in recrystallized feldspar and muscovite. We conclude that at the given metamorphic conditions apatite is open for Sr isotope reequilibration, most likely due to dynamic recrystallization during mylonitization. We suggest that apatite can be independently used also for dating deformation in mylonites that do not contain feldspar, e.g., in mica-bearing quartzitic mylonites.

The NNE-trending Kyshtym strike-slip fault in the Middle Urals demonstrates an orogen-parallel mass transfer in the Middle Urals. The evolution of the fault is characterized by a stage of ductile deformation followed by a stage of brittle faulting. The maximum total displacement is estimated at 43±15 km. Rb–Sr dating of mylonites suggests that ductile shearing occurred between ~250 and ~240 Ma. The Late Permian/Early Triassic age is surprising as longitudinal mass transfer has previously not been considered to play a significant role during the Permo-Triassic orogenic phase of the Urals. We interpret the dextral strike-slip fault to reflect the lateral mass transfer along the southeastern margin of an indenter belonging to the East European craton. Sinistral transcurrent faults that have reworked the Main Uralian fault may represent conjugate faults along the northeastern margin of the indenter.

Acknowledgements R. Hetzel gratefully acknowledges invaluable logistical support and introduction to the field by V. Lennykh from the Mineralogical Institute in Miass, Russian Academy of Sciences. We thank J. Müller and M. Langanke for help with sample preparation. Discussions with H. Echtler and A. Plesch at an early stage of this work are greatly appreciated. U. Riller and D. Hindle are thanked for critically reading a previous version of the manuscript. Careful and constructive

reviews by U. Giese, C. Juhlin, and U. Kramm are gratefully acknowledged. This project was financially supported by the Deutsche Forschungsgemeinschaft (grant no. EC 138/3–1/2) and the GeoForschungsZentrum (GFZ) Potsdam.

References

Ayarza P, Brown D, Alvarez-Marron J, Juhlin C (2000) Contrasting tectonic history of the arc-continent suture in the Southern and Middle Urals: implications for the evolution of the orogen. J Geol Soc Lond 157:1065–1076

Belkovski AI (1989). Symplectite-eclogites of the middle Urals. USSR Acad Sci, Sverdlovsk (in Russian)

Blanckenburg F von, Villa IM, Baur H, Morteani G, Steiger RH (1989) Time calibration of a PT-path from the Western Tauern Window, Eastern Alps: the problem of closure temperatures. Contrib Mineral Petrol 101:1–11

Brown D, Alvarez-Marron J, Pérez-Estaun A, Gorozhanina Y, Baryshev V, Puchkov V (1997) Geometric and kinematic evolution of the foreland thrust and fold belt in the southern Urals. Tectonics 16:551–562

Brown D, Juhlin C, Alvarez-Marron J, Pérez-Estaun A, Oslianski A (1998) Crustal-scale structure and evolution of an arc-continent collision zone in the southern Urals, Russia. Tectonics 17:158–171

Burke K, Sengör AMC (1986) Tectonic escape in the evolution of the continental crust. Geodyn Series 14:41–53

Clauer N, O'Neill JR, Bonnot-Courtois C (1982) The effect of natural weathering on the chemical and isotopic compositions of biotites. Geochim Cosmochim Acta 46:1755–1762

Dewey JF, Hempton MR, Kidd WSF, Saroglu F, Sengör AMC (1986) Shortening of continental lithosphere: the neotectonics of Eastern Anatolia: a young collision zone. Geol Soc Lond Spec Publ 19:3–36

Dodson MH (1973) Closure temperature in cooling geochronological and petrological systems. Contrib Mineral Petrol 40:259–274

Dunlap WJ (1997) Neocrystallization or cooling? $^{40}Ar/^{39}Ar$ ages of white micas from low-grade mylonites. Chem Geol 143:181–203

Echtler HP, Hetzel R (1997) Main Uralian Thrust and Main Uralian Normal Fault: non-extensional Palaeozoic high-P rock exhumation, oblique collision, and normal faulting in the Southern Urals. Terra Nova 9:158–162

Echtler HP, Ivanov KS, Ronkin YL, Karsten LA, Hetzel R, Noskov AG (1997) The tectono-metamorphic evolution of gneiss complexes in the Middle Urals, Russia: a reappraisal. Tectonophysics 276:229–251

Eide EA, Echtler HP, Hetzel R, Ivanov KS (1997) Cooling age diachroneity and Paleozoic orogenic processes in the Middle and Southern Urals. Terra Nova 9 (Abstr Suppl 1):119

Freeman SR, Inger S, Butler RWH, Cliff RA (1997) Dating deformation using Rb–Sr in white mica: greenschist facies deformation ages from the Entrelor shear zone, Italian Alps. Tectonics 16:57–76

Giese U, Glasmacher U, Kozlov VI, Matenaar I, Puchkov VN, Stroink L, Bauer W, Ladage S, Walter R (1999) Structural framework of the Bashkirian anticlinorium, SW Urals. Geol Rundsch 87:526–544

Glasmacher UA, Reynolds P, Alekseyev AA, Puchkov VN, Taylor K, Gorozhanin V, Walter R (1999) $^{40}Ar/^{39}Ar$ thermochronology west of the Main Uralian fault, southern Urals, Russia. Geol Rundsch 87:515–525

Hames WE, Bowring SA (1994) An empirical evaluation of the argon diffusion geometry in muscovite. Earth Planet Sci Lett 124:161–169

Hamilton W (1970) The Uralides and the motion of the Russian and Siberian Platforms. Geol Soc Am Bull 81:2553–2576

Hetzel R (1999) Geology and geodynamic evolution of the high-P/low-T Maksyutov Complex, southern Urals, Russia. Geol Rundsch 87:577–588

Hetzel R, Romer RL (1999) U–Pb dating of the Verkniy Ufaley intrusion, Middle Urals, Russia: a minimum age for subduction and amphibolite facies overprint of the East European continental margin. Geol Mag 136:593–597

Hetzel R, Echtler HP, Seifert W, Schulte BA, Ivanov KS (1998) Subduction- and exhumation-related fabrics in the Paleozoic high-pressure/low-temperature Maksyutov Complex, Antingan area, southern Urals, Russia. Geol Soc Am Bull 110:916–930

Huchon P, Le Pichon X, Rangin C (1994) Indochina peninsula and the collision of India and Eurasia. Geology 22:27–30

Ivanov SN, Perfiliev AS, Efimov AA, Smirnov GA, Necheukhin VM, Fershtater GB (1975) Fundamental features in the structure and evolution of the Urals. Am J Sci 254:107–136

Jäger E (1973) Die alpine Orogenese im Lichte der radiometrischen Altersbestimmung. Eclogae Geol Helvet 66:11–21

Kazantseva TT, Kamaletdinov MA (1986) The geosynclinal development of the Urals. Tectonophysics 127:371–381

Keilman GA (1974) Migmatite complexes of the mobile belts. Nedra, Moscow, pp 1–198 (in Russian)

Kisters AFM, Meyer FM, Seravkin IB, Znamensky SE, Kosarev AM, Ertl RGW (1999) The geological setting of lode-gold deposits in the central southern Urals: a review. Geol Rundsch 87:603–616

Kramm U, Blaxland AB, Kononova VA, Grauert B (1983) Origin of the Ilmenogorsk-Vishnevogorsk nepheline syenites, Urals, USSR, and their time of emplacement during the history of the Ural fold belt: a Rb–Sr study. J Geol 91:427–435

Kramm U, Chernyshev IV, Grauert B, Kononova VA, Brücker W (1993) Zircon typology and U–Pb systematics: a case study of zircons from Nepheline Syenite of the Il'meny Mountains, Urals. Petrology 1:474–485

Kühn A, Glodny J, Iden K, Austrheim H (2000) Retention of Precambrian Rb/Sr phlogopite ages through Caledonian eclogite facies metamorphism, Bergen Arc Complex, W-Norway. Lithos 51:305–330

Lennykh VI (1963) The age of the metamorphic rocks in the Uraltau zone. Proc of the Commission for Defining the Absolute Age of Geological Formations. USSR Acad Sci 11:253–264 (in Russian)

Levin VY (1974) The Ilmenogorsk-Vishnevogorsk alkaline province. Nauka, Moscow, pp 1–222 (in Russian)

Ludwig KR (1999) Isoplot/Ex Version 2.06. Berkeley Geochronology Center. Spec Publ 1a, Berkeley, California

Meyer B, Tapponier P, Gaudemer Y, Peltzer G, Shunmin G, Zhitai C (1996) Rate of left-lateral movement along the easternmost segment of the Altyn Tagh fault, east of 96°E (China). Geophys J Int 124:29–44

Müller W, Dallmeyer RD, Neubauer F, Thöni M (1999) Deformation-induced resetting of Rb/Sr and $^{40}Ar/^{39}Ar$ mineral systems in a low-grade, polymetamorphic terrane (Eastern Alps, Austria). J Geol Soc Lond 156:261–278

Neumann W, Huster E (1974) The half-life of ^{87}Rb measured as difference between the isotopes ^{87}Rb and ^{85}Rb. Z Phys 270:121–127

Passchier CW, Trouw RAJ (1996) Microtectonics. Springer, Berlin Heidelberg New York, pp 1–289

Peltzer G, Tapponier P (1988) Formation and evolution of strike-slip faults, rifts, and basins during the India–Asia collision: an experimental approach. J Geophys Res 93:15085–15117

Peltzer G, Tapponier P, Gaudemer Y, Meyer B, Shunmin G, Kelun Y, Zhitai C, Huagung D (1988) Offsets of late Quarternary morphology, rate of slip, and recurrence of large earthquakes on the Chang Ma fault (Gansu, China). J Geophys Res 93:7793–7812

Pfiffner OA, Ramsay JG (1982) Constraints on geological strain rates: arguments from finite strain states of naturally deformed rocks. J Geophys Res 87:311–321

Pryer LL (1993) Microstructures in feldspars from a major crustal thrust zone: the Grenville Front, Ontario, Canada. J Struct Geol 15:21–36
Puchkov VN (1997) Structure and geodynamics of the Uralian orogen. In: Burg JP, Ford M (eds) Orogeny through time. Geol Soc Lond Spec Publ, pp 201–236
Ramsay JG (1967) Folding and fracturing of rocks. McGraw-Hill, New York, pp 1–568
Ramsay JG, Graham RH (1970) Strain variation in shear belts. Can J Earth Sci 7:786–813
Ratschbacher L, Frisch W, Linzer H-G, Merle O (1991) Lateral extrusion tectonics in the Eastern Alps. Part 2. Structural analysis. Tectonics 10:257–271
Reddy SM, Potts GJ (1999) Constraining absolute deformation ages: the relationship between deformation mechanisms and isotope systematics. J Struct Geol 21:1255–1265
Ronenson BM (1966) The origin of miaskites and the associated rare-metal mineralizations. Ser Geol 28:1–174 (in Russian)
Sieh K, Jahns RH (1984) Holocene activity of the San Andreas fault at Wallace Creek, California. Geol Soc Am Bull 95:883–896
Sobolev ID (1986) Geological map of the northern, middle and northeastern part of the southern Urals. Scale: 1:1,000,000, Geol Surv USSR and Ural Geol Committee
Stöckhert B, Brix MR, Kleinschrodt R, Hurford AJ, Wirth R (1999) Thermochronometry and microstructures of quartz: a comparison with experimental flow laws and predictions on the temperature of the brittle-plastic transition. J Struct Geol 21:351–369
Tapponnier P, Molnar P (1976) Slip-line field theory and large-scale continental tectonics. Nature 264:319–324
Tapponnier P, Peltzer G, Le Dain AY, Armijo R, Cobbold PR (1982) Propagating extrusion tectonics in Asia: new insights from simple experiments with plasticine. Geology 10:611–616
Twiss RJ, Moores EM (1992) Structural geology. Freeman, New York, pp 1–532
Villa IM (1998) Isotopic closure. Terra Nova 10:42–47
Zonenshain LP, Korinevsky VG, Kazmin VG, Pechersky DM, Khain VV, Matveenkov VV (1984) Plate tectonic model of the South Urals development. Tectonophysics 109:95–135